Annals of Anatomy 218 (2018) 205–212

Contents lists available at ScienceDirect

Annals of Anatomy

journal homepage: www.elsevier.com/locate/aanat

Normal microscopic anatomy of equine body and limb skin: A morphological and immunohistochemical study☆

Elin Jørgensen[a], Giulia Lazzarini[b], Andrea Pirone[b], Stine Jacobsen[a], Vincenzo Miragliotta[b,*]

[a] Department of Veterinary Clinical Sciences, University of Copenhagen, Højbakkegaard Alle 5, DK-2630 Taastrup, Denmark
[b] Department of Veterinary Sciences, University of Pisa, viale delle Piagge 2, 56124 Pisa, Italy

ARTICLE INFO

Article history:
Received 19 October 2017
Received in revised form 12 March 2018
Accepted 29 March 2018

Keywords:
Horse
Skin
Differentiation markers
Epithelial thickness
Proliferation index
Mast cells

ABSTRACT

Introduction: Information on microscopic anatomy of equine skin is sparse. In horses, limb wounds often become chronic and/or non-healing whereas body wounds heal normally. These dissimilarities in healing patterns might be a product of different phenotypic characteristics of body and limb skin. The objective of this study was to investigate microscopic anatomy, epidermal thickness, keratinocyte proliferation and differentiation as well as the presence of mast cells in normal equine skin of body and limb.
Materials and methods: The study involved body and limb skin biopsies from six horses. Histological characteristics of the epidermis were assessed and epithelial thickness measured. Immunohistochemistry was performed to investigate epidermal differentiation patterns of cytokeratin (CK) 10, CK14, CK16, loricrin, and peroxisome proliferator-activated receptor alpha (PPAR-α), epidermal proliferation (Ki-67 immunostaining), and mast cells distribution in the skin.
Results: The epidermis was significantly thicker in the limb skin compared to body skin ($p < 0.01$). Epidermal proliferation and CK distribution did not show differences in the two anatomical areas. Loricrin presence was focally found in the spinous layer in four out of six limb skin samples but not in body skin samples. Tryptase positive mast cells were detected in the dermis and their density (cell/mm^2) was not different between body and limb.
Discussion and conclusion: Here we report for the first time about the normal distribution of CK10, CK14, CK16, PPAR-α, and loricrin in equine limb and body skin as well as about epidermal proliferation rate and mast cell count. It will be relevant to investigate the distribution of the investigated epithelial differentiation markers and the role of mast cells during equine wound healing and/or other skin diseases.

1. Introduction

Skin is a complex organ that contains several cell populations (Jatana and DeLouise, 2014). The microscopic anatomy of equine skin is poorly described with the most prominent work published more than 40 years ago (Talukdar et al., 1972a,b).

Horses are prone to different skin diseases like traumatic wounds, sarcoids, tumors, allergies and atopy (Wobeser, 2015). Difficult-to-heal wounds are common among horses (Owen et al., 2012; Theoret et al., 2016) and were in 2015 estimated to account for 16% of euthanasia in adult horses in the US (Anon, 2015). Specifically, healing of wounds located in the metacarpal/metatarsal area in horses is often fraught with complications compared to wounds located at the body (Jorgensen et al., 2017; Sørensen et al., 2014; Theoret et al., 2001). Impaired wound healing in equine limb wounds is characterized with greater retraction, premature cessation of contraction, slower rates of epithelialization, and formation of exuberant granulation tissue (Hendrickson and Virgin, 2005; Theoret and Wilmink, 2013). The chronic healing pattern seen in equine limb wounds is a complex and multifactorial process, as several factors seem to contribute. These factors include hypoxia (Sørensen, 2014), persistent chronic inflammation (Bundgaard et al., 2016; Wilmink et al., 1999), presence of biofilm (Jorgensen et al., 2017) and differential gene/protein expression (Miragliotta et al., 2008a,b, 2009). *In vitro* studies showed that fibroblasts from equine limb skin have dissimilar responses to different growth factors than fibroblast from the oral mucosa, which might be contributing to the different healing responses at these locations (Rose, 2012; Watts and Rose, 2012). It is possible that also

☆ This paper belongs to the special issue Animal Anatomy III.
* Corresponding author.
E-mail address: vincenzo.miragliotta@unipi.it (V. Miragliotta).

https://doi.org/10.1016/j.aanat.2018.03.010
0940-9602/

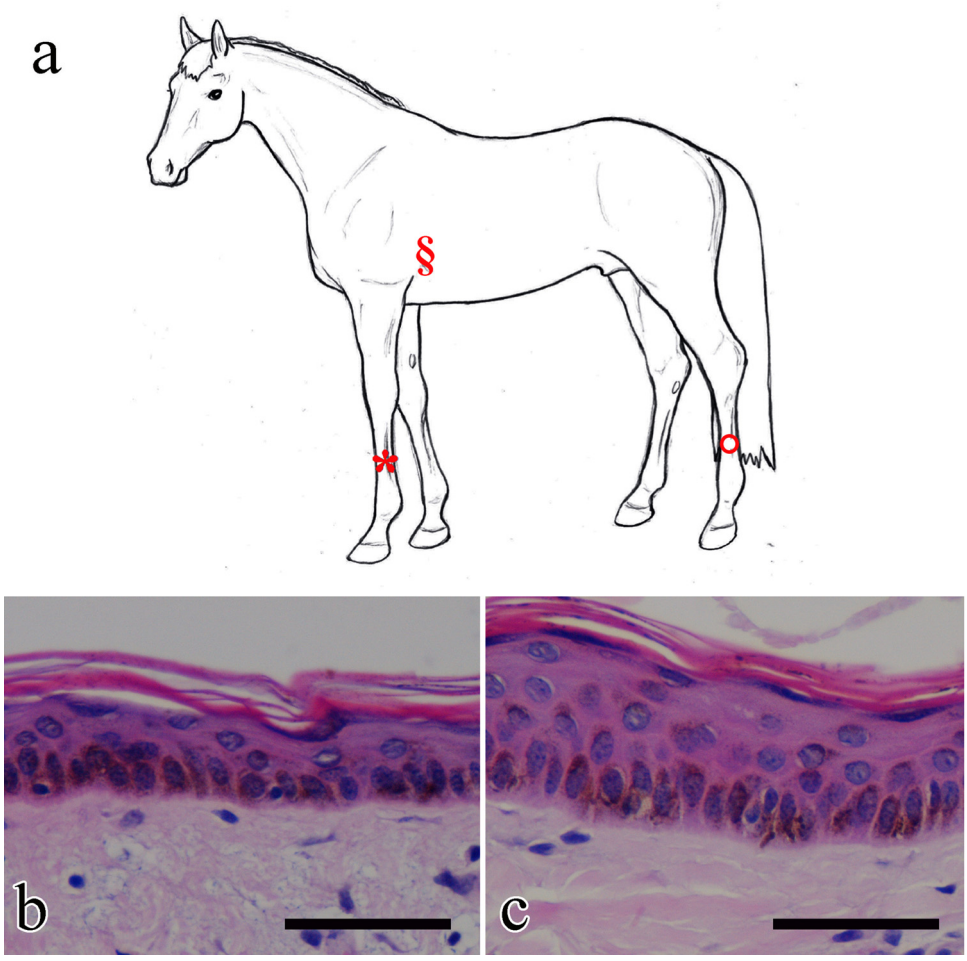

Fig. 1. Drawing illustrating the sampling site (a) and hematoxylin and eosin stained sections of equine body (b) and limb (c) skin showing different thickness of epidermis. Symbols in (a) indicate where skin was sampled from the six horses: § = thorax just caudal to the triceps muscle; * = lateral metacarpus, ° = lateral metatarsus. Scale bars in (b) and (c) are equal to 50 μm.

other anatomical/phenotypical differences might contribute to the differences observed during wound repair.

To improve our understanding of equine skin conditions and wound healing it is thus important to obtain more information on the microanatomy and to understand how normal keratinocytes differentiate and proliferate in equine skin at different locations. Keratinocyte differentiation can be dissected by immunostaining of different cytokeratins and other proteins specifically expressed by either undifferentiated (basal) or more differentiated (suprabasal) cells (Abramo et al., 2016). Very little is known about expression of these differentiation markers in equine skin, but results from other species indicate that Cytokeratin (CK) 14 is present in basal and early suprabasal cells (Castagnoli et al., 2010; Kobayashi et al., 2013), CK10 is specifically present in suprabasal cells (Abramo et al., 2016), CK16 is expressed by activated keratinocytes in humans (Freedberg et al., 2001), and that loricrin is a stratum granulosum protein involved in terminal differentiation and formation of the stratum corneum (Liang et al., 2012). Furthermore, peroxisome proliferator-activated receptor-α (PPAR-α) was selected for its reported role in the re-epithelialization process (Michalik et al., 2001).

The objective of this study was thus to characterize the normal microscopic anatomy of body and limb skin of horses. Descriptive morphology and immunohistochemistry were used to investigate epidermal thickness, keratinocyte proliferation rate, expression of CK10, CK14, CK16, loricrin, PPAR-α, and distribution of mast cells.

2. Materials and methods

2.1. Animals and samples

Eight millimeter skin punch biopsies were collected from six adult geldings weighing 430–500 kg. The horses were clinically healthy and were without any signs or history of dermatological diseases or injuries. The mantle color of the horses was bay (three horses), black (two horses), and strawberry roan (one horse). The horses were sedated and received local analgesia before the biopsies were obtained. Samples were obtained from the lateral metacarpus (mid cannon), lateral metatarsus (mid cannon), and from the thorax just caudal to the triceps muscle as indicated in Fig. 1a. The samples were placed in 4% formaldehyde for fixation before embedding in paraffin wax. The experimental protocol was approved by the Danish Animal Experiments Inspectorate (license no. 2016-15-0201-00981), and procedures were carried out as per the Danish Animal Testing Act and the EU Directive 2010/63/EU for animal experiments.

2.2. General morphology and epidermal thickness

For histological evaluation and epidermal thickness measurements body, front, and hind limb skin sample sections stained with haematoxylin and eosin were used. The sections were first evaluated by light microscopy for qualitative assessment of morphological features (epidermis, pigment, hair follicles, seba-

Table 1
Primary and secondary antibodies used for immunohistochemical analyses.

Primary antibodies

Name	Company	Number	Clonality	Host	Dilution
Anti-CK16	Cloud-Clone corp.	PAA516Hu01	Polyclonal	Rabbit	1:200
Anti-CK14	Abcam	Ab7800	Monoclonal	Mouse	1:200
Anti-CK10	Abcam	Ab9026	Monoclonal	Mouse	1:200
Anti-Loricrin	Abcam	Ab24722	Polyclonal	Rabbit	1:400
Anti-Ki-67	Dako	M7240	Monoclonal	Mouse	1:300
Anti-PPAR-α	Novusbio	NBP1-03288	Polyclonal	Rabbit	1:200
(Anti-Mast Cell Tryptase (AA1))	Santa Cruz Biotechnology	sc-59587	Monoclonal	Mouse	1:400

Secondary antibodies

Name	Company	Number	Host	Dilution
DyLight649 Anti-mouse IgG	Vector Laboratories	DI-2649	Horse	1:200
DyLight488 Anti-mouse IgG	Vector Laboratories	DI-2488	Horse	1:200
DyLight488 Anti-rabbit IgG	Vector Laboratories	DI-1088	Horse	1:200
R.T.U. biotinylated universal antibody anti-rabbit/mouse	Vector Laboratories	BP-1400	Horse	RTU

ceous glands, sweat glands, and dermis). Epidermal thickness was measured as previously reported by Abramo et al. (2016). Briefly, ten images were collected at 400× magnification; 16 measures were recorded for each image by manually tracing the extent of the epidermis with NIS-Elements Br Microscope Imaging Software (NIS-Elements Br Microscope Imaging Software, Nikon Instruments, Calenzano, Italy). The traced thicknesses were perpendicular to the basement membrane and extended from the basement membrane to the beginning of the stratum corneum.

2.3. Immunohistochemical analyses of skin samples

Sections (4 μm) were cut and deparaffinized using a standardized method by immersing the glass slides in xylene (3 × 5 min), 99% ethanol (2 × 5 min), 95% ethanol (2 × 5 min), 70% ethanol (1 × 5 min), and in distilled water (2 × 5 min). To investigate the spatial distribution of CK10, CK14, CK16, loricrin, and PPAR-α indirect immunofluorescence was performed. For Ki-67 (cell proliferation marker) and mast cell tryptase, sections were stained by the immunoperoxidase method. All commercial antibodies used are displayed in Table 1.

Primary antibodies were applied after heat-induced epitope retrieval, 1% hydrogen peroxide treatment (only for immunoperoxidase method), and standard blocking. Antibodies were left for 19 h at 4 °C. After washing in PBS (4 × 10 min) secondary antibodies were applied for one hour. After washing in PBS (3 × 10 min) sections for fluorescence were mounted with a mounting media containing DAPI (Vectashield® Hard Set mounting media with DAPI, Vector Laboratories, Burlingame, California) and sections for peroxidase had ABC reagent (Vectastain® R.T.U Elite® ABC reagent, Vector Laboratories, Burlingame, California) applied for 45 min at room temperature. After another wash in PBS (3 × 10 min) the peroxidase sections were developed using DAB reagent (ImmPACT™ DAB peroxidase substrate kit, Vector Laboratories, Burlingame, California) for 120 s. After that, sections were dehydrated in increasing alcohol gradients, cleared in xylene and mounted with permanent mounting medium (DPX mountant for microscopy, BDH – VWR International Ltd., Poole, England). Immunohistochemistry was performed on hind limb and body samples, but not on front limb samples, as no differences in general morphology and epidermal thickness were discovered between front and hind limb skin.

The epidermal proliferation index (Ki-67 immunostaining) was calculated after counting the number of positively stained basal keratinocytes related to the number of total basal keratinocytes throughout the skin biopsy. Values were expressed as percent of positive cells out of the total basal cells.

Microscopic examinations of immunofluorescence tissue sections were performed by using a fluorescence microscope (Nikon Eclipse 80i, Nikon Instruments, Calenzano, Italy) and the accompanying software (NIS-Elements Br Microscope Imaging Software, Nikon Instruments, Calenzano, Italy).

2.4. Mast cell distribution

As described in Section 2.3, immunohistochemistry was performed on body and limb skin samples with the primary antibody against mast cell tryptase. Mast cell distribution was evaluated under a standard light microscope (Nikon Ni-e, Nikon Instruments, Calenzano, Italy) at ×100 magnification using the accompanying software (NIS-Elements Br Microscope Imaging Software, Nikon Instruments, Calenzano, Italy). The positive cells were counted in two different areas of the dermis in accordance with a previously reported method (van der Haegen et al., 2001): the subepidermal layer (here defined as 0–325 μm below the basal membrane) and the deep dermis (325–975 μm below the basal membrane), and were expressed as number of cells/mm^2.

2.5. Statistical analysis

All data handling was done using Microsoft Excel 2010, and paired t-tests and one way ANOVA analyses were performed using GraphPad Prism version 5.01 (GraphPad Software, San Diego California, USA). Data are reported as means ± SD. Mast cell tryptase positive cells data are presented as median (range) and analyzed using Wilcoxon signed rank test in SAS Enterprise Guide 7.13 (SAS Institute Inc., Cary, NC, USA). A significance level of $p < 0.05$ was chosen for this study.

3. Results

3.1. General morphology, epidermal thickness and keratinocyte proliferation

Stratum basale, stratum spinosum, stratum granulosum and stratum corneum were present in both body and limb skin samples. Melanin pigment was confined to the stratum basale. Two-four and four-six layers of keratinocytes were countable in body and limb skin, respectively (Fig. 1b,c). The average epidermal thickness of skin was 29.36 μm ± 3.58 μm for the body, 46.22 μm ± 7.84 μm for hind limbs, and 46.76 μm ± 6.31 μm for front limbs. There was a statistically significant difference between body and limb epidermal thickness ($p < 0.01$), but no significant difference between hind limb and front limb epidermal thickness ($p = 0.10$).

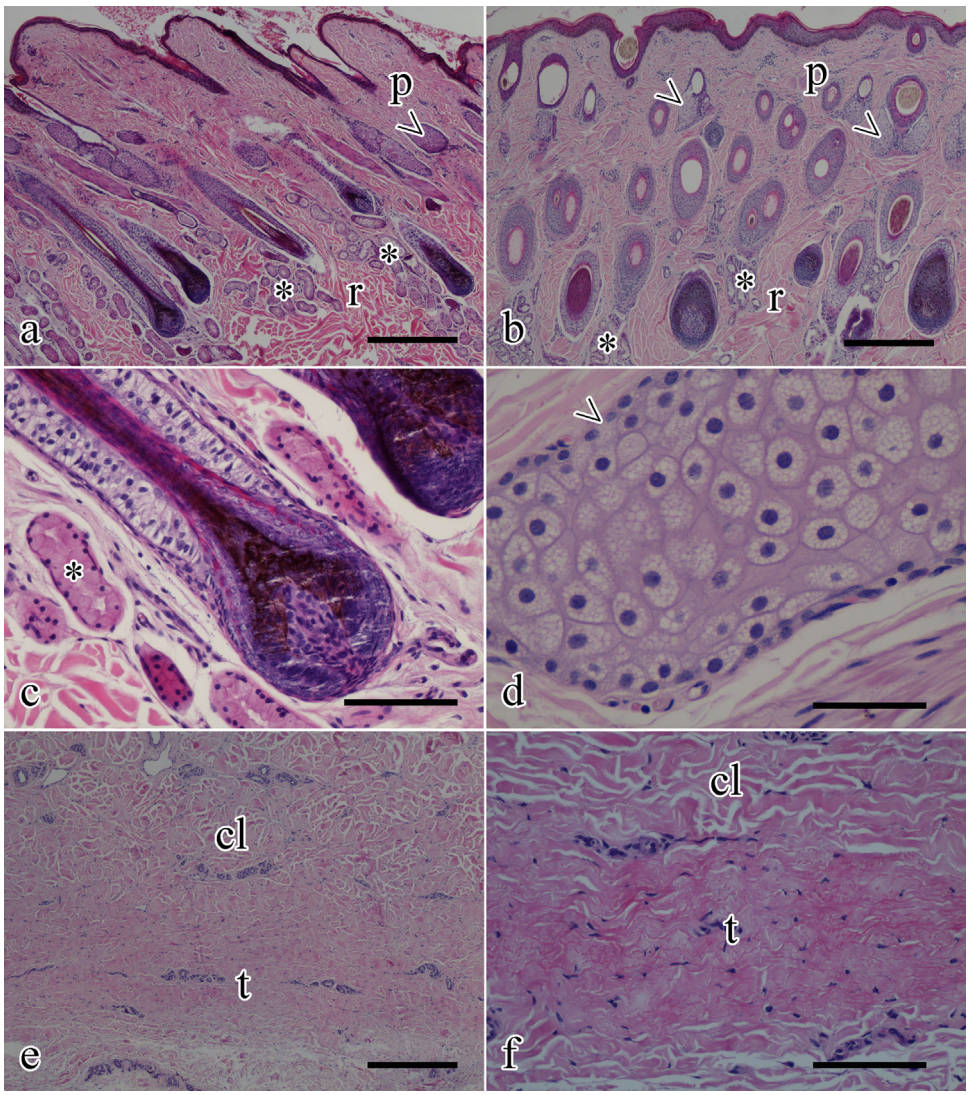

Fig. 2. Hematoxylin and eosin stained sections of equine body (a) and limb (b) skin: p = papillary dermis, r = reticular dermis; arrowheads indicate sebaceous glands and asterisk indicate apocrine sweat glands. (c) High magnification of a hair bulb in the anagen phase of cycling; asterisk indicate apocrine sweat gland. (d) High magnification of a sebaceous gland showing a multivacuolated cytoplasm with centrally located nucleus. (e-f) Low and high magnification respectively of the deep dermis of limb skin showing the cordovan layer (cl) and the third/accessory layer (t). Scale bars are equal to 400 μm (a, b, e), 100 μm (c–d), or 50 μm (f).

The epidermal proliferation indices for body and limb skin were 7.42 ± 2.33 and 6.78 ± 3.16, respectively, which did not differ statistically significantly ($p = 0.69$).

Hair follicles were primarily in the anagen phase. Arrector pili muscles, sebaceous glands, and sweat glands were present in all samples. Sebaceous glands showed a multivacuolated cytoplasm with nuclei located centrally. The dermis showed the presence of thinner collagen bundles in the subepidermal area (papillary dermis) compared to thicker bundles seen in the underlying parts (reticular dermis). Below the reticular dermis a cordovan layer was observed in both areas while, in limb samples only, collagen bundles became thicker and formed an accessory layer (namely the third/accessory layer). Collagen bundle orientation in the accessory layer was parallel to the epidermal surface. These histological findings are displayed in Fig. 2. No pathological changes were observed in any of the samples.

3.2. Epidermal differentiation markers

CK10 was found in keratinocyte suprabasal layers only (spinosum and granulosum). CK14 was found in stratum basale keratinocytes as well as in the stratum spinosum, where the staining fainted. CK16 was found in all epithelial structures (epidermis, sweat and sebaceous glands, epithelial structures of hair follicles); in the epidermis, staining was most prominent in the basal and suprabasal keratinocytes. PPAR-α was found in the stratum basale of the epidermis, in endothelial cells, and in perivascular subepidermal cells. CK10, CK14, CK16 and PPAR-α were always observed as cytoplasmic staining. These findings were similar for body and limb skin. Loricrin also showed a cytoplasmic localization and was present in the stratum granulosum only in body skin, but in limb skin multifocal areas with loricrin extending into the stratum spinosum were found in 4 out of 6 horses (67%). Immunohistochemical findings are displayed in Fig. 3.

3.3. Mast cell distribution

In the subepidermal layer 54.3 (18.2–101.1) mast cells/mm^2 were found in body samples and 38.1 (2.4–103.7) mast cells/mm^2 were found in limb samples, there was no statistical difference between the different areas ($p = 0.59$). In the deeper dermis 21.7 (8.6–38.4) mast cells/mm^2 were found in body samples and 23.9

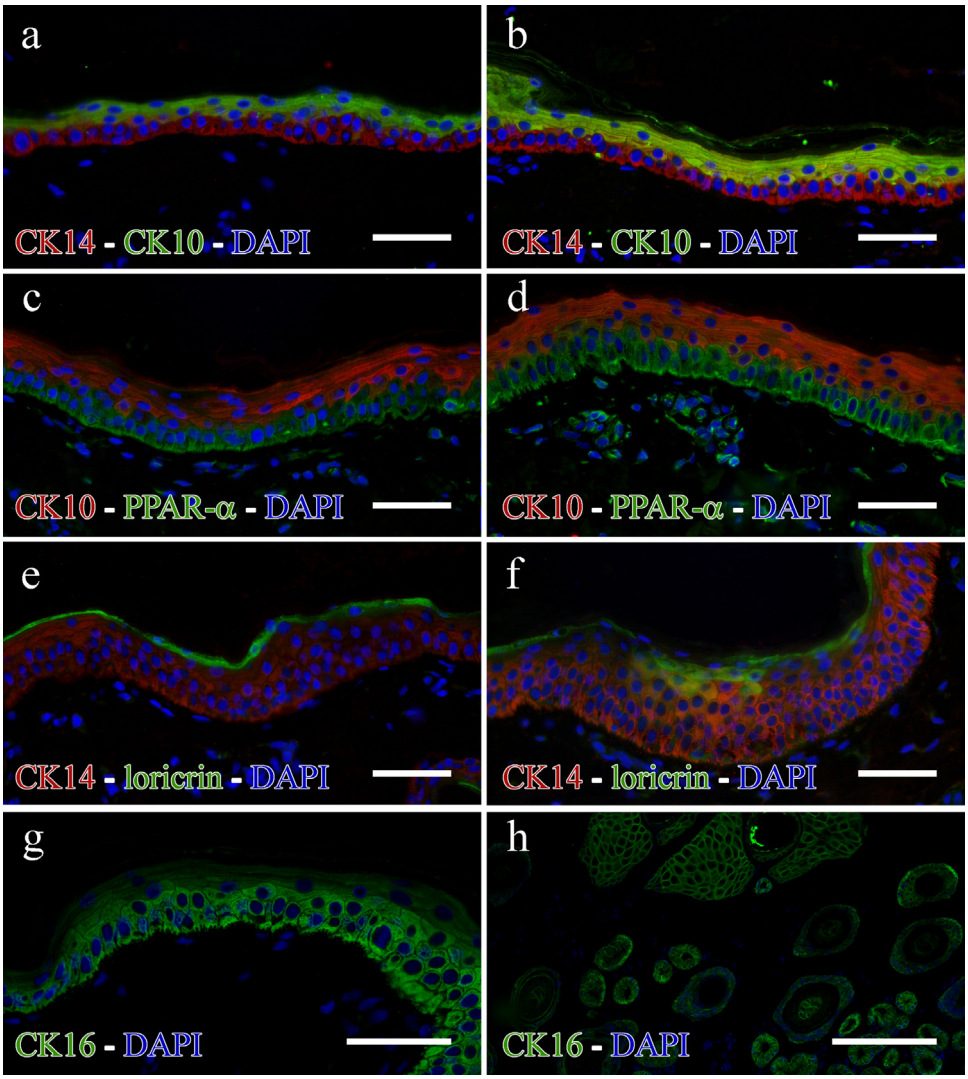

Fig. 3. Immunostaining of equine skin samples with cytokeratin (CK)10, CK14, CK16, loricrin and PPAR-α. Left images are from body skin samples while right images are from limb skin. Different colors are explained within the figure. (a–g) Epidermal immunostaining: CK10 is detected in all the suprabasal layers (spinosum, granulosum and corneum); CK14 is mainly expressed in the stratum basale while it faints suprabasally; loricrin specifically stains the stratum granulosum; PPAR-α is present only in the basal keratinocytes. (h) CK16 positivity in the epithelial structures of the dermis (hair follicles, sebaceous, and sweat glands). Scale bars are equal to 50 μm (a–f) or 200 μm (h).

(15.0–32.5) mast cells/mm^2 were found in limb samples, there was no statistical difference between the different areas ($p = 0.81$). Taken together, there were significantly more mast cell tryptase positive cells per mm^2 in the subepidermal layer than in the deeper dermal layer ($p = 0.04$). Representative images of tryptase immunohistochemistry are shown in Fig. 4.

4. Discussion

Skin samples included in the study showed normal skin morphology similar to that reported previously (Talukdar et al., 1972a). Equine dermal microscopic structure has been studied by other investigators: the different appearance of collagen fibers described in the present study can be referred to the papillary (superficial) dermis, reticular dermis, cordovan layer and third/accessory cordovan layer (Wakuri et al., 1995). The latter was found exclusively in limb samples in our study. It is not clear how localization of the accessory cordovan layer in equine skin could affect pathological responses in the skin.

In 1972, Talukdar et al. investigated epidermal thickness of different body areas from 13 horses using an ocular micrometer, but unfortunately, the study did not assess metacarpal or metatarsal epidermal thickness. The thickness of the body epidermis (in the costal region) was 46 μm, i.e. considerably thicker that the 29.36 μm recorded for thoracic skin in our study. These differences can be due to different equipment and techniques used for the measurements, and/or could be related to breed differences. The horses examined in our study were mixed breed warmblood horses, while the breed of the horses in the study by Talukdar et al. (1972a,b) was not mentioned. The consequences of the thicker epidermis observed in the equine limb compared to that of body skin need to be evaluated, but it may affect stiffness/elasticity of the skin and thereby retraction and contraction of skin in wound healing since, as reported earlier (Wakuri et al., 1995), it comprises elastic fibers interwoven to collagen fibers.

Cytokeratins are important structural proteins of the cytoskeleton of epithelial cells. The keratinocyte differentiation markers CK10 and CK14 were expressed in the suprabasal layers (spinosum, granulosum and corneum) and in the stratum basale of the epidermis, respectively. This distribution was expected based on previous reports (Pastar et al., 2014). CK 14 was present also in the suprabasal layers characterized by a fainted staining. This is in line with human skin where basal layer cells express CK14 (Porter et al., 2000) and

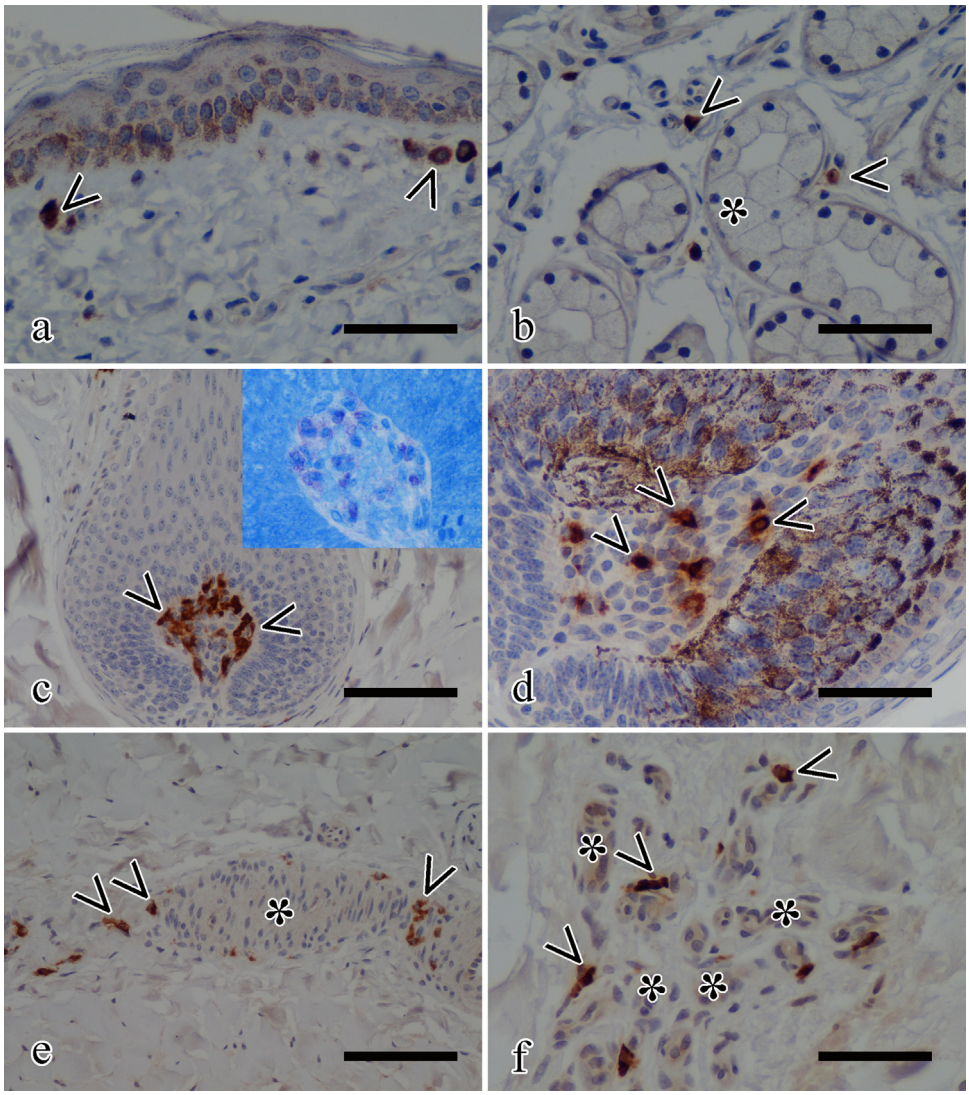

Fig. 4. Tryptase immunostaining for mast cells, representative images from body (a, b) and limb (c–f) skin. (a) Subepidermal mast cells indicated by arrowheads. (b) Arrowheads indicate mast cells intercalated to apocrine sweat glands (asterisk). (c–d) Low and high magnification respectively of a hair bulb focusing on the hair papilla were several mast cells are visible (indicated by arrowheads). Inset in (c) shows toluidine blue stained mast cells within hair papilla. (e–f) Third/accessory cordovan layer vascular plexuses (asterisks) with perivascular mast cells (arrowheads). Scale bars are equal to 50 μm (a, b, d, f) or 100 μm (c, e).

rapidly turn on the expression of CK10 during differentiation while gradually decreasing CK14 gene transcription (Woodcock-Mitchell et al., 1982; Fuchs, 1995). In skin from horses suffering from chronic pastern dermatitis with moderate to marked epidermal hyperplasia, abnormal keratinocyte differentiation was evident with decreased expression of CK10 and CK14 in the suprabasal and basal layers, respectively, and increased expression of CK14 in the suprabasal layers (Geburek et al., 2005). These findings indicate that expression patterns of cytokeratin are changed during skin disease in horses. Surprisingly, CK16 was present in normal epithelia, which is contrary to human skin, where CK16 is a "stress" CK found only in activated keratinocytes in the epidermis as part of the wound healing process or during hyperproliferation (Freedberg et al., 2001; Jiang et al., 1993). Species-differences in "stress" CK expression was demonstrated previously, as Walter (2001) demonstrated CK6, expressed only in activated cells in human skin (Galvin et al., 1989; Mckay and Leigh, 1995), to be present in basal and suprabasal layers of normal canine skin. These species differences could reflect the tension placed on skin, the presence of CK16 in skin has been suggested to be a stabilization mechanism against increased load (Jiang et al., 1993; Walter, 2001), which may be higher in horses than in humans.

As loricrin is a terminal differentiation marker, it was detected as expected in the stratum granulosum of the epidermis (Liang et al., 2012). However, multifocal dystrophic deposits in deeper layers were observed in four out of six limb skin samples. Loricrin has a defensive and protective function in the epidermis (Nithya et al., 2015). The expression of loricrin is increased in a group of disorders (palmo plantar keratoderma) in humans, where hyperkeratosis occurs on soles and palms; in patients suffering from these disorders loricrin is expressed in more cell layers than normal (Nithya et al., 2015). Multifocal dystrophic loricrin deposits in deeper layers of the equine limb epidermis could be a sign of increased stress and loading of the skin in this area, but could also be an artifact caused by oblique sectioning of hair follicles in limb skin, as these contain loricrin in their walls. Future studies should investigate this by staining skin section cut strictly parallel to the epidermal surface.

PPAR-α is a nuclear receptor that regulates metabolism. As reported for human skin (Westergaard et al., 2003), PPAR-α was found in the cytoplasm of the basal keratinocytes in equine skin.

While its functions have never been investigated in horses, PPAR-α is down-regulated in atopic dermatitis and some skin cancers in humans (Sertznig et al., 2008). Also in a murine wound model PPAR was described to play a role in re-epithelialization (Michalik et al., 2001).

The epidermal proliferation index has not been reported in horses before, but expression of Ki-67 has been used to document proliferation in an equine *in vitro* skin model (Cerrato et al., 2014) and in stem cell treatment of equine wounds (Broeckx et al., 2014). In human and veterinary medicine, the epidermal proliferation (Ki-67) index has been used to diagnose and prognosticate skin tumors (Marinescu et al., 2016), including canine and equine mast cell tumors (Halse et al., 2014; Maglennon et al., 2008). The normal epidermal proliferation (Ki-67) index of equine skin reported here can be used as normal value in diagnostic equine dermatology.

The amount of mast cell tryptase positive cells per mm^2 in the different compartments of the skin in this study was very much in line with findings of van der Haegen et al. (2001), where biopsies from the mane/tale base were analyzed. Also in canine skin, more mast cells are present in the subepidermal dermis compared to deeper dermis (Auxilia and Hill, 2000). The presence of tryptase positive mast cells in the subepidermal dermis has been associated with delayed wound healing and epithelialization in a human study (Huttunen et al., 2000). Involvement in equine healing should be further investigated, but as equine body and limb skin contained similar numbers of tryptase positive mast cells, it does not seem likely that they contribute to the delayed wound healing of equine limb wounds.

In conclusion, despite a larger study involving a higher number of horses may be warranted to draw general conclusions, our work may serve as a basis for further investigations aimed to explore changes occurring in epidermal thickness, keratinocyte proliferation/differentiation and mast cell count during wound healing and other dermatopathological conditions affecting horses.

Sources of funding

E.J. was funded by a Danish Government PhD grant, and the work was supported by the Augustinus foundation. The funding sources had no involvement on the research or the preparation of the manuscript.

Acknowledgement

Anti-CK16 was generously sponsored by Cloud-Clone Corp. (provided by DBA Italia srl).

References

Anon. Equine 2015, Section 1C: Baseline Reference of Equine Health and Management in the United States 2015. United States Department of Agriculture, Fort Collins, CO, USA, 2016. https://www.aphis.usda.gov/animal_health/nahms/equine/downloads/equine15/Eq2015_Rept1.pdf (Accessed 10 October 2017).

Abramo, F., Pirone, A., Lenzi, C., Vannozzi, I., Della Valle, M.F., Miragliotta, V., 2016. Establishment of a 2-week canine skin organ culture model and its pharmacological modulation by epidermal growth factor and dexamethasone. Ann. Anat. 207, 109–117.

Auxilia, S.T., Hill, P.B., 2000. Mast cell distribution, epidermal thickness and hair follicle density in normal canine skin: possible explanations for the predilection sites of atopic dermatitis? Vet. Dermatol. 11, 247–254.

Broeckx, S.Y., Maes, S., Martinello, T., Aerts, D., Chiers, K., Marien, T., Patruno, M., Franco-Obregon, A., Spaas, J.H., 2014. Equine epidermis: a source of epithelial-like stem/progenitor cells with in vitro and in vivo regenerative capacities. Stem Cells Dev. 23, 1134–1148.

Bundgaard, L., Bendixen, E., Sorensen, M.A., Harman, V.M., Beynon, R.J., Petersen, L.J., Jacobsen, S., 2016. A selected reaction monitoring-based analysis of acute phase proteins in interstitial fluids from experimental equine wounds healing by secondary intention. Wound Repair Regen. 24, 525–532.

Castagnoli, C., Fumagalli, M., Alotto, D., Cambieri, I., Casarin, S., Ostorero, A., Casimiri, R., Germano, P., Pezzuto, C., Stella, M., 2010. Preparation and characterization of a novel skin substitute. J. Biomed. Biotechnol., http://dx.doi.org/10.1155/2010/840363, Article ID 840363.

Cerrato, S., Ramio-Lluch, L., Brazis, P., Rabanal, R.M., Fondevila, D., Puigdemont, A., 2014. Development and characterization of an equine skin-equivalent model. Vet. Dermatol. 25, 475–477.

Freedberg, I.M., Tomic-Canic, M., Komine, M., Blumenberg, M., 2001. Keratins and the keratinocyte activation cycle. J. Invest. Dermatol. 116, 633–640.

Fuchs, E., 1995. Keratins and the skin. Annu. Rev. Cell Dev. Biol. 11, 123–153.

Galvin, S., Loomis, C., Manabe, M., Dhouailly, D., Sun, T.T., 1989. The major pathways of keratinocyte differentiation as defined by keratin expression: an overview. Adv. Dermatol. 4, 277–299.

Geburek, F., Ohnesorge, B., Deegen, E., Doeleke, R., Hewicker-Trautwein, M., 2005. Alterations of epidermal proliferation and cytokeratin expression in skin biopsies from heavy draught horses with chronic pastern dermatitis. Vet. Dermatol. 16, 373–384.

Halse, S., Pizzirani, S., Parry, N.M., Burgess, K.E., 2014. Mast cell tumor invading the cornea in a horse. Vet. Ophthalmol. 17, 221–227.

Hendrickson, D., Virgin, J., 2005. Factors that affect equine wound repair. Vet. Clin. North Am. Equine Pract. 21, 33–44.

Huttunen, M., Aalto, M.L., Harvima, R.J., Horsmanheimo, M., Harvima, I.T., 2000. Alterations in mast cells showing tryptase and chymase activity in epithelializating and chronic wounds. Exp. Dermatol. 9, 258–265.

Jatana, S., DeLouise, L.A., 2014. Understanding engineered nanomaterial skin interactions and the modulatory effects of ultraviolet radiation skin exposure. Wiley Interdiscip. Rev. Nanomed. Nanobiotechnol. 6, 61–79.

Jiang, C.K., Magnaldo, T., Ohtsuki, M., Freedberg, I.M., Bernerd, F., Blumenberg, M., 1993. Epidermal growth factor and transforming growth factor alpha specifically induce the activation- and hyperproliferation-associated keratins 6 and 16. Proc. Natl. Acad. Sci. U. S. A. 90, 6786–6790.

Jorgensen, E., Bay, L., Bjarnsholt, T., Bundgaard, L., Sorensen, M.A., Jacobsen, S., 2017. The occurrence of biofilm in an equine experimental wound model of healing by secondary intention. Vet. Microbiol. 204, 90–95.

Kobayashi, T., Enomoto, K., Wang, Y.H., Yoon, J.S., Okamura, R., Ide, K., Ohyama, M., Nishiyama, T., Iwasaki, T., Nishifuji, K., 2013. Epidermal structure created by canine hair follicle keratinocytes enriched with bulge cells in a three- dimensional skin equivalent model in vitro: implications for regenerative therapy of canine epidermis. Vet. Dermatol. 24, 77–83, e19–20.

Liang, X., Bhattacharya, S., Bajaj, G., Guha, G., Wang, Z., Jang, H.S., Leid, M., Indra, A.K., Ganguli-Indra, G., 2012. Delayed cutaneous wound healing and aberrant expression of hair follicle stem cell markers in mice selectively lacking Ctip2 in epidermis. PLoS One 7, e29999.

Maglennon, G.A., Murphy, S., Adams, V., Miller, J., Smith, K., Blunden, A., Scase, T.J., 2008. Association of Ki67 index with prognosis for intermediate-grade canine cutaneous mast cell tumours. Vet. Comp. Oncol. 6, 268–274.

Marinescu, A., Stepan, A.E., Margaritescu, C., Marinescu, A.M., Zavoi, R.E., Simionescu, C.E., Niculescu, M., 2016. P53, p16 and Ki67 immunoexpression in cutaneous squamous cell carcinoma and its precursor lesions. Rom. J. Morphol. Embryol. 57, 691–696.

Mckay, I.A., Leigh, I.M., 1995. Altered keratinocyte growth and differentiation in psoriasis. Clin. Dermatol. 13, 105–114.

Michalik, L., Desvergne, B., Tan, N.S., Basu-Modak, S., Escher, P., Rieusset, J., Peters, J.M., Kaya, G., Gonzalez, F.J., Zakany, J., Metzger, D., Chambon, P., Duboule, D., Wahli, W., 2001. Impaired skin wound healing in peroxisome proliferator-activated receptor (PPAR)alpha and PPARbeta mutant mice. J. Cell Biol. 154, 799–814.

Miragliotta, V., Ipina, Z., Lefebvre-Lavoie, J., Lussier, J.G., Theoret, C.L., 2008a. Equine CTNNB1 and PECAM1 nucleotide structure and expression analyses in an experimental model of normal and pathological wound repair. BMC Physiol. 8, 1.

Miragliotta, V., Lefebvre-Lavoie, J., Lussier, J.G., Theoret, C.L., 2008b. Equine ANXA2 and MMP1 expression analyses in an experimental model of normal and pathological wound repair. J. Dermatol. Sci. 51, 103–112.

Miragliotta, V., Raphäel, K., Lussier, J.G., Theoret, C.L., 2009. Equine lumican (LUM) cDNA sequence and spatio-temporal expression in an experimental model of normal and pathological wound healing. Vet. Dermatol. 20 (4), 243–248.

Nithya, S., Radhika, T., Jeddy, N., 2015. Loricrin – an overview. J. Oral Maxillofac. Pathol. 19, 64–68.

Owen, K.R., Singer, E.R., Clegg, P.D., Ireland, J.L., Pinchbeck, G.L., 2012. Identification of risk factors for traumatic injury in the general horse population of north-west England, Midlands and north Wales. Equine Vet. J. 44, 143–148.

Pastar, I., Stojadinovic, O., Yin, N.C., Ramirez, H., Nusbaum, A.G., Sawaya, A., Patel, S.B., Khalid, L., Isseroff, R.R., Tomic-Canic, M., 2014. Epithelialization in wound healing: a comprehensive review. Adv. Wound Care 3, 445–464.

Porter, R.M., Lunny, D.P., Ogden, P.H., Morley, S.M., McLean, W.H.I., Evans, A., Harrison, D.L., Rugg, E.L., Lane, E.B., 2000. K15 expression implies lateral differentiation within stratified epithelial basal cells. Lab. Invest. 80, 1701–1710.

Rose, M.T., 2012. Effect of growth factors on the migration of equine oral and limb fibroblasts using an in vitro scratch assay. Vet. J. 193, 539–544.

Sertznig, P., Seifert, M., Tilgen, W., Reichrath, J., 2008. Peroxisome proliferator-activated receptors (PPARs) and the human skin: importance of PPARs in skin physiology and dermatologic diseases. Am. J. Clin. Dermatol. 9, 15–31.

Sørensen, M.A., 2014. Hypoxia as a Cause of Exuberant Granulation Tissue Formation in Equine Limb Spunds Healing by Second Intention, Faculty of Health and Medical Science. University of Copenhagen.

Sørensen, M.A., Pedersen, L.J., Bundgaard, L., Toft, N., Jacobsen, S., 2014. Regional disturbances in metabolism and blood flow in equine limb wounds healing with formation of exuberant granulation tissue. Wound Repair Regen. 22, 647–653.

Talukdar, A.H., Calhoun, M.L., Stinson, A.W., 1972a. Microscopic anatomy of the skin of the horse. Am. J. Vet. Res. 33, 2365–2390.
Talukdar, A.H., Calhoun, M.L., Stinson, A.W., 1972b. Specialized vascular structure in the skin of the horse. Am. J. Vet. Res. 33, 335–338.
Theoret, C.L., Barber, S.M., Moyana, T.N., Gordon, J.R., 2001. Expression of transforming growth factor β1, β3, and basic fibroblast growth factor in full-thickness skin wounds of equine limbs and thorax. Vet. Surg. 30, 269–277.
Theoret, C.L., Bolwell, C.F., Riley, C.B., 2016. A cross-sectional survey on wounds in horses in New Zealand. N. Z. Vet. J. 64, 90–94.
Theoret, C.L., Wilmink, J.M., 2013. Aberrant wound healing in the horse: Naturally occurring conditions reminiscent of those observed in man. Wound Repair Regen. 21, 365–371.
van der Haegen, A., Griot-Wenk, M., Welle, M., Busato, A., von Tscharner, C., Zurbriggen, A., Marti, E., 2001. Immunoglobulin-E-bearing cells in skin biopsies of horses with insect bite hypersensitivity. Equine Vet. J. 33, 699–706.
Wakuri, H., Mutoh, K., Ichikawa, H., Liu, B., 1995. Microscopic anatomy of the equine skin with special reference to the dermis. Okajimas Folia Anat. Jpn. 72, 177–183.
Walter, J.H., 2001. Cytokeratins in the canine epidermis. Vet. Dermatol. 12, 81–87.
Watts, E.J., Rose, M.T., 2012. Extracellular matrix expression by equine oral and limb fibroblasts in in vitro culture. Res. Vet. Sci. 92, 213–218.
Westergaard, M., Henningsen, J., Johansen, C., Rasmussen, S., Svendsen, M.L., Jensen, U.B., Schroder, H.D., Staels, B., Iversen, L., Bolund, L., Kragballe, K., Kristiansen, K., 2003. Expression and localization of peroxisome proliferator-activated receptors and nuclear factor kappaB in normal and lesional psoriatic skin. J. Invest. Dermatol. 121, 1104–1117.
Wilmink, J.M., Van Weeren, P.R., Stolk, P.W.T., Van Mil, F.N., Barneveld, A., 1999. Differences in second-intention wound healing between horses and ponies: histological aspects. Equine Vet. J. 31, 61–67.
Wobeser, B.K., 2015. Skin diseases in horses. Vet. Clin. North Am. Equine Pract. 31, 359–376.
Woodcock-Mitchell, J., Eichner, R., Nelson, W.G., Sun, T.T., 1982. Immunolocalization of keratin polypeptides in human-epidermis using monoclonal-antibodies. J. Cell Biol. 95, 580–588.